

Energetic study of ultrasonic wettability enhancement

Jon Ander Sarasua^{a,*}, Leire Ruiz Rubio^b, Estibaliz Aranzabe^a, Jose Luis Vilas Vilela^b

^a *Tekniker, Basque Research and Technology Alliance (BRTA), C/Inaki Goenaga 5, 20600 Eibar, Spain*

^b *Grupo de Química Macromolecular (LQM) Dpto. Química Física, Facultad de Ciencia y Tecnología, Universidad del País Vasco (UPV/EHU), 48940 Leioa, Spain*

ARTICLE INFO

Keywords:

Wettability
Ultrasound
Acoustic energy
Contact angle

ABSTRACT

Many industrial and biological interfacial processes, such as welding and breathing depend directly on wettability and surface tension phenomena. The most common methods to control the wettability are based on modifying the properties of the fluid or the substrate. The present work focuses on the use of high-frequency acoustic waves (ultrasound) for the same purpose. It is well known that ultrasound can effectively clean a surface by acoustic cavitation, hence ultrasonic cleaning technology. Besides the cleaning process itself, many authors have observed an important wettability enhancement when liquids are exposed to low and high (ultrasonic) frequency vibration. Ultrasound goes one step further as it can instantly adjust the contact angle by tuning the vibration amplitude, but there is still a lack of comprehension about the physical principles that explain this phenomenon. To shed light on it, a thermodynamic model describing how ultrasound decreases the contact angle in a three-phase wetting system has been developed. Moreover, an analytical and experimental research has been carried out in order to demonstrate that ultrasound is an important competitor to surfactants in terms of energy efficiency and environmental friendliness.

1. Introduction

Both humans and nature profit from wettability or contact angle modification for different purposes, for example cleaning. Among other methods, surface texturing and chemical surface tension modification (surfactants) prevail. For cleaning applications, high intensity ultrasonic technology has demonstrated to be a strong competitor of surfactants. The current state of the art confirms that the process is mainly based on the mechanical dragging of acoustic cavitation [1]. The physics of ultrasonic cleaning have been widely studied by authors such as Lauterborn [2–4] and Mason [5] who concluded that the bubble size, number and distribution depend mainly on the ultrasonic parameters (amplitude and frequency) and the liquid itself (volume, surface tension, density and viscosity). However, there is a collateral phenomenon that several authors [6,7] have observed: the contact angle is modified when the liquids are exposed to low and high frequency vibration. This paper considers high frequency as ultrasonic (non-audible) frequency which is above the threshold of 20 000 Hz. To avoid a grey area and considering the research of other authors, the low frequency regime will be located below 200 Hz (100 times lower).

In the second context, there are many studies that analyse how liquid droplets react when exposed to vibration. The combination of the bulk

vibration and the surface capillary waves conform an eigenvalue problem, that was solved by Lamb's [8] Eq. (1):

$$\omega = \sqrt{\frac{\gamma}{3\pi m}(n-1)(n+2)} \quad (1)$$

This equation describes the resonant frequencies (ω) of a liquid droplet as a function of its surface tension (γ), mass (m) and an integer number (n). With the advance in computational fluid dynamic (CFD) simulation techniques, not only the resonant frequencies but also the modal shape of the droplet has been predicted by authors such as Dong [9] and Tamura [10]. They studied the vibration modes of a sessile water droplet under vibration. Fig. 1 shows how droplets react when vibration is applied on the substrate. The droplet will adopt different vibration shapes depending on the input frequency. The low frequency vibration modes are visible to the naked eye and the contact angle is variable along the perimeter [7].

For high frequency vibration, capillary waves are so small that it becomes difficult to appreciate the periodic oscillation of the contact angle (Fig. 2). Indeed, high frequency surface waving can only be appreciated when the amplitude is high enough to distort the reflection of the light. If the input amplitude exceeds certain thresholds, atomization will take place, and therefore, it becomes impossible to retain the

* Corresponding author.

E-mail address: jonander.sarasua@tekniker.es (J.A. Sarasua).

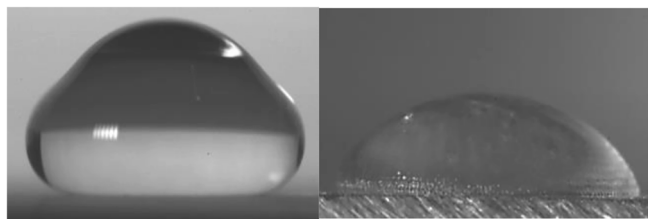


Fig. 1. Example of low (28 Hz, left) and high (20196 Hz, right) frequency vibration modes.

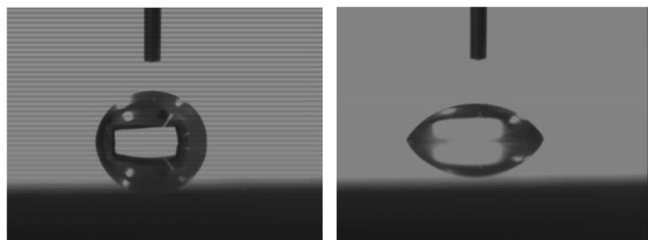


Fig. 2. Initial contact angle (left) and decrease (right) on distilled water under 20 kHz vibration. No capillary waves are observed.

droplet on the surface (it is jetted and broken into thousands of microdroplets, losing in this way the liquid phase). For the present work, this amplitude threshold represents the maximum wettability enhancement under stable conditions. The foresaid phenomenon has been studied by many authors, such as Lang [11], who experimentally obtained the following Eq. (2), which predicts the atomized droplet's diameter (D) depending on the surface tension (γ), the density (ρ) and the frequency (f).

$$D = 0.68 \left(\frac{\pi\gamma}{\rho f^2} \right)^{1/3} \quad (2)$$

As can be observed, D is inversely proportional to the frequency, which means that higher frequencies lead to the formation of smaller droplets. Regarding the atomization threshold, many authors such as Pohlman [12], Sorokin [13] and Lozano et al. [14] have obtained empirical Eqs. (3) to estimate the atomization amplitude (a) as a function of the foresaid properties and the kinematic viscosity (η).

$$a = \frac{2\eta}{\rho} \left(\frac{\rho}{\pi\gamma f} \right)^{1/3} \quad (3)$$

If the foresaid thresholds are not exceeded, the vibration of the droplet will be stable and its behaviour can be predicted [15] with a dynamic contact angle. However, this prediction becomes more difficult when working at high frequency. When the vibration frequency exceeds 20 kHz (ultrasonic regime), the dynamic surface deformation is almost imperceptible, and the contact angle becomes apparently constant. For wetting systems, the vibration reduces the contact angle [16]. That is, ultrasonic vibration induces an instantaneous increase of wettability. Morozov and Manor [17] conclude that this phenomenon is related to cavitation and the increase of temperature between phases, but Lin [18] does not observe changes in temperature. Manor [19] described a vibration driving force at megasonic frequency (1 MHz) observing an increase of the contact angle for non-wetting systems such as water-PTFE. In his work, Manor [19] formulated the vibration driving force (F) as Eq. (4), where (r) is the base radius of the droplet and (θ) is the contact angle. This driving force is derived from the internal streaming that takes place under mega sonic vibration frequency, where the wavelength is shorter than the size of the droplet.

$$F \approx \frac{\rho}{32\sqrt{\frac{2\eta}{\rho f}}} r^2 (fa)^2 \cos(\theta)^2 \quad (4)$$

From the same equation, Lin [18] predicts the resulting contact angle reduction ($\Delta\theta$) by Eq. (5):

$$\Delta\theta \approx \frac{\rho}{\gamma 32\sqrt{\frac{2\eta}{\rho f}}} r^2 (\omega a)^2 \cos(\theta)^2 \quad (5)$$

This theory fits very well with the research of Trapuzzano [6,20], who observed that by modifying the vibration amplitude, the contact angle can be modulated.

With the aim of increasing the knowledge beyond the state of the art, the present work will focus on the one hand on describing how the driving force reduces the contact angle in a three-phase wetting system. Unlike previous authors, the analytical approach will be based on the thermodynamic balance of the whole system under ultrasonic conditions, where the wavelength is greater than the size of the droplet. On the other hand, the work will compare the efficiency of ultrasonic wettability enhancement to conventional methods (heat and chemical surfactants).

2. Analytical study

A water droplet deposited on a solid metallic surface composes a three-phase system as shown in Fig. 3: gas (air), liquid (water) and solid (metal). After the deposition, the interfacial forces find the balance for a certain contact angle as defined by Young's Eq. (6), where (γ_{SG}), (γ_{SL}) and γ correspond to the solid-gas, solid-liquid, and gas-liquid inter-phase surface tension, respectively.

$$\cos\theta = \frac{\gamma_{SG} - \gamma_{SL}}{\gamma} \quad (6)$$

The contact angle(θ) is therefore a magnitude that describes the way in which the liquid phase wets the solid phase. The lower it gets, the more spreading there will be. From the previous equation could be concluded that the only way to modify its value is modifying the different interfacial tension or γ values. This equation does not consider the influence of external forces. It is obvious that if the edge of the droplet is mechanically pulled, the contact angle will be reduced. This is what it happens, for instance, when the solid substrate is tilted and the gravity pulls one side of the droplet.

However, once this external force is removed, the droplet should return to its original shape, but in a wetting system, it does not. Indeed, the same droplet can find the internal balance for different contact angles. This phenomenon is called contact angle hysteresis and does not apply only to constant forces, but also to harmonic ones [19].

If a droplet on a solid surface is exposed to a harmonic axial force (perpendicular), one or several vibration modes will be excited, so the

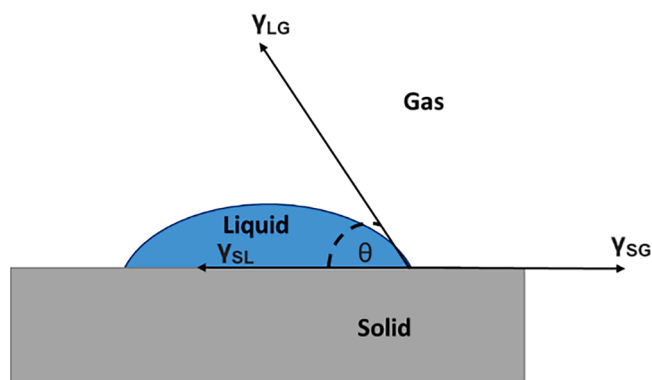


Fig. 3. Three-phase system and contact angle.

droplet will vibrate deforming its shape. If the force is tangential (parallel) the droplet will also vibrate, but other vibration modes will be excited. This research did not consider tangential vibration, as it tends to displace the droplet.

On non-wetting systems, the cohesive forces are so low that the contact surface will be expanded and shrunken periodically (Fig. 4). Therefore, the continuous measurement on a goniometer will conclude that the contact angle oscillates periodically. Nevertheless, in wetting systems, when the droplet is expanded, it can no longer retract. The expansive part of the acoustic wave will enlarge the surface of the droplet and therefore reduce the contact angle. The resting part of the wave will shrink the surface, but the contact angle hysteresis will oppose to this part of the driving force, avoiding the angle recovery (Fig. 5). The present study considers the cases where the contact angle hysteresis is strong enough to avoid the contact line withdrawal.

Considering a single surface A, the global energy balance is expressed with Eq. (7), where (dU) is the differential internal energy, (T) the temperature, (dS) the differential entropy, (P) the pressure, (dV) the differential volume, (dA) the differential interfacial surface, (μ) the chemical potential and (dN) the molar differential of the different (i) phases.

$$dU = TdS - PdV + \sum \gamma_i dA_i + \sum \mu_i dN_i \quad (7)$$

For an incompressible liquid without chemical exchange, only the entropic and surface energy components remain in the Eq. (7). Dividing the surface energy term on its main three interfacial components, the previous equation yields to Eq. (8):

$$dU = TdS + \gamma_{SL}dB - \gamma_{SG}dB + \gamma dA \quad (8)$$

The first T dS term represents the entropic losses, B the base area of the droplet and A the gas liquid interface area. The different γ are the surface energy density values of each interphase. At constant room temperature and atmospheric pressure, all γ terms can be considered constant [21]. The shape of a droplet is described as a spherical cap whose geometrical parameters are summarized in Fig. 6.

If an external energy source is introduced, a liquid droplet has the potential to increase its surface, but not its volume (volume conservation principle). Considering the geometrical parameters of an spherical cap (Fig. 6) and introducing Young's Eq. (6), Eq. (8) is integrated obtaining Eq. (9):

$$\frac{\Delta U}{\gamma} = (1 - \cos\theta_0) \left(\frac{2V_0}{h} - \pi \frac{h^2}{3} - B_0 \right) - \pi(h_0^2 - h^2) \quad (9)$$

Before applying the vibration, the initial volume (V_0), the contact angle (θ_0) and the height (h_0) are known parameters (initial state of the droplet). For the Eq. (9) the only unknown terms are the resulting height

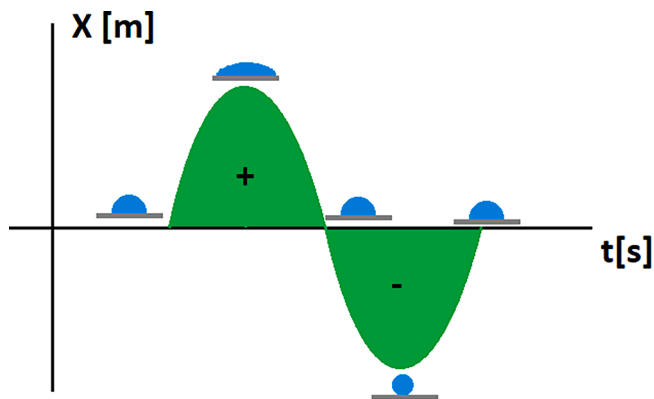


Fig. 4. Displacement generated by a low-frequency acoustical wave. If no contact angle hysteresis exists, the contact angle would oscillate around maximum and minimum values.

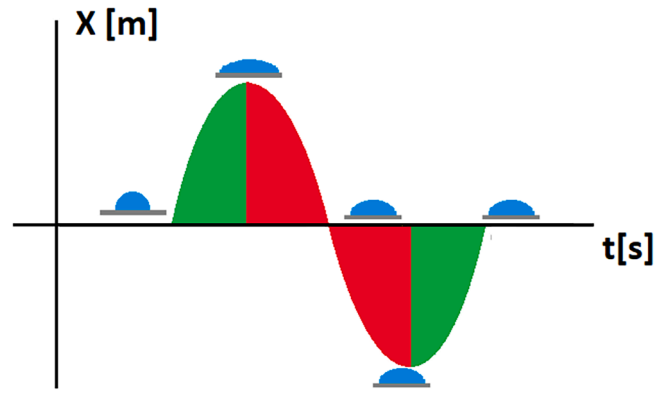


Fig. 5. Displacement generated by an acoustical wave. Due to hysteresis, the contact does not recover its original value. Only the expansive side of the wave modifies the surface area.

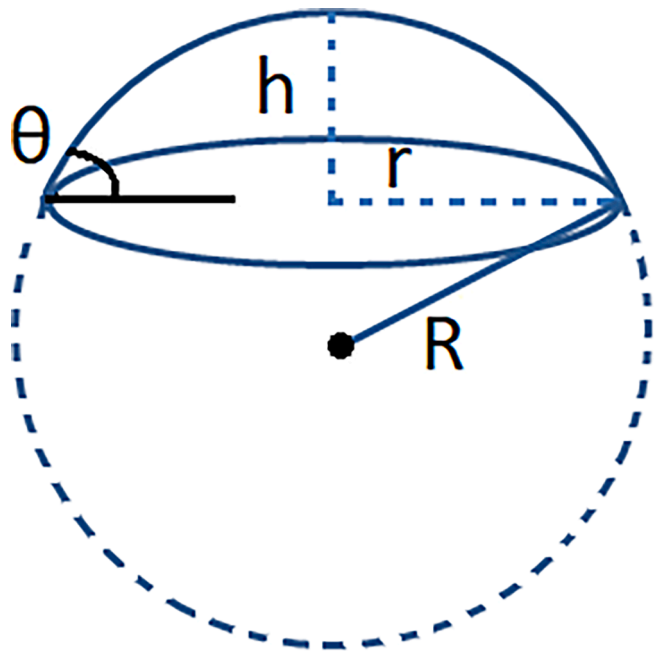


Fig. 6. Main geometrical parameters of a spherical cap.

(h) of the droplet after applying the vibration and the amount of acoustic energy ΔU introduced into the system. The equation refers to an ideal scenario where all the introduced energy turns into surface energy. The increase of entropy will be studied during the experimental part of the work.

The acoustic energy density (W), can expressed by Eq. (10):

$$W = \rho(a\omega)^2 \quad (10)$$

Considering that only the expansive part is responsible for the generation of a new surface ΔU can be expressed as:

$$\Delta U = \frac{\rho V_0 (a\omega)^2}{\gamma} \quad (11)$$

Introducing this energy function (10) into Eq. (9), it turns into Eq. (11), where the only unknown term is the final height h of the droplet.

$$\frac{\rho V_0 (a\omega)^2}{2\gamma} = (1 - \cos\theta_0) \left(\frac{2V_0}{h} - \pi \frac{h^2}{3} - B_0 \right) - \pi(h_0^2 - h^2) \quad (12)$$

With the volume and height of a droplet, all the rest geometrical parameters (contact angle, contact surface and radius) can be directly

obtained through the geometric equations that describe a spherical cap. In conclusion, if the initial geometry of the droplet, the vibration amplitude and the frequency are known, the present model can predict the final shape of the droplet. Fig. 7 shows an example of resolving the equation for a water droplet exposed to 20 kHz of vibration at different amplitudes. The Newton-Raphson algorithm has been programmed in Matlab© for numerical solving.

3. Experimental procedure

3.1. Validation of the thermodynamic model

The experimental procedure is focused, on the one hand, on validating the model for different fluids and substrates and, on the other hand, on comparing the ultrasonic wettability increase to conventional methods (heat and surfactants). For the validation of the proposed models, a 60 W Bandelin Sonoplus HD 2200 homogenization equipment with a 20 kHz blade sonotrode has been used. All the experiments have been performed on the back side of the sonotrode (low amplitude side) with the aim of reaching 100% of the nominal acoustic power without atomization. The vibration amplitude of the equipment is usually not linearly proportional to the power, so it has been measured with a Keyence LK-G82 50 kHz laser system as shown in Fig. 8.

Once the amplitude has been measured, the ultrasonic wettability enhancement has been characterized through the contact angle. An optical goniometer OEG Surfrens Universal has been used for this purpose, as shown in Fig. 9. After each experiment, the solid surface has been cleaned with ethanol.

As expressed in Eq. (8), internal friction might heat the liquids and therefore the interfacial tension will vary. To check that said heat does not modify the surface tension, a National Instruments© thermocouple has been used to monitorize the temperature during the contact angle measurements (Fig. 10 and Fig. 11). The device detects up to 0.1 °C of temperature variation.

3.2. Comparison with conventional methods

On the other hand, the ultrasonic wettability enhancement has been compared to traditional methods (thermal and chemical). The thermal method has been characterized by means of a laboratory heating plate, the thermocouple, and the optical goniometer.

Regarding the chemical method, different water and SDBS (sodium dodecylbenzenesulfonate) concentrations have been characterized with the optical goniometer and a Kruss© K20 (100 µg resolution) surface tension measurement equipment. As an exothermic reaction, the dissolution of SDBS in water releases heat, so the temperature increase of the solution has also been controlled with the thermocouple.

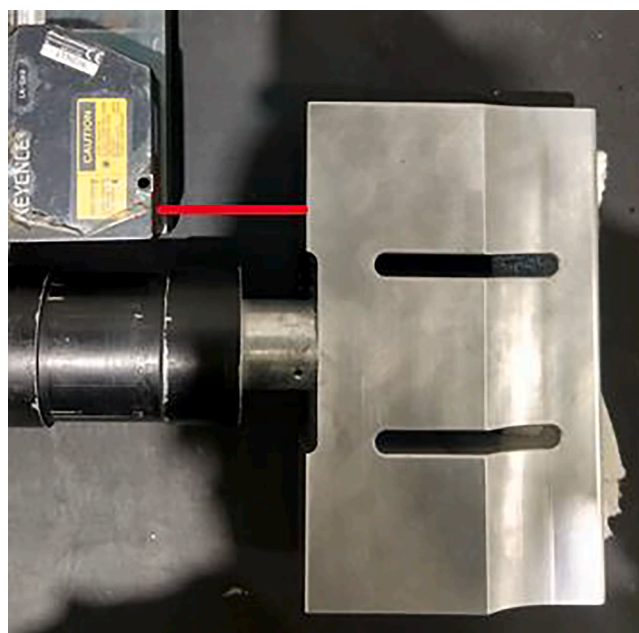


Fig. 8. Amplitude measurement of the backside of the sonotrode.

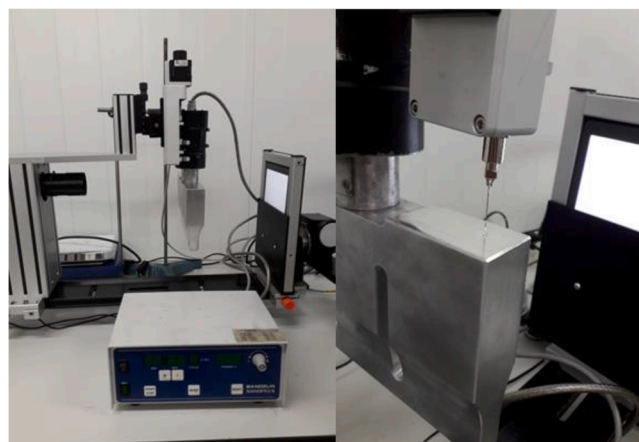


Fig. 9. Ultrasonic equipment assembled on optical goniometer.

4. Results and discussion

4.1. Validation of the models

From the initial laser measurements, it can be concluded that the power-amplitude relationship is not linear (Table 1). Therefore, only the

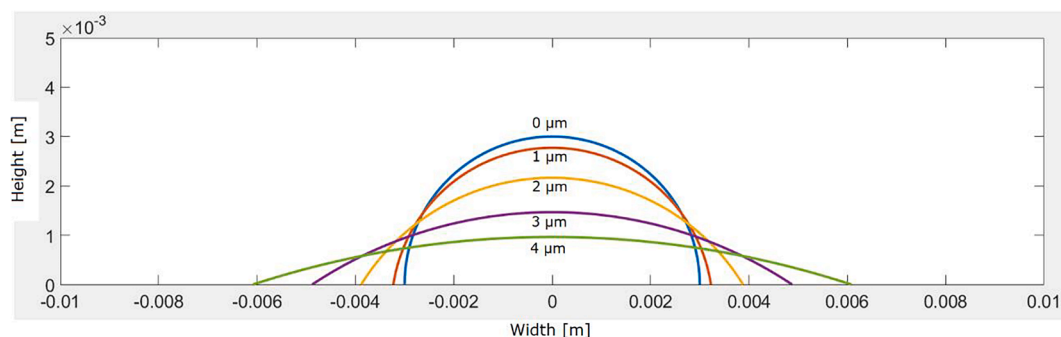


Fig. 7. Resulting shape of a water droplet for different sound amplitudes at 20 kHz.

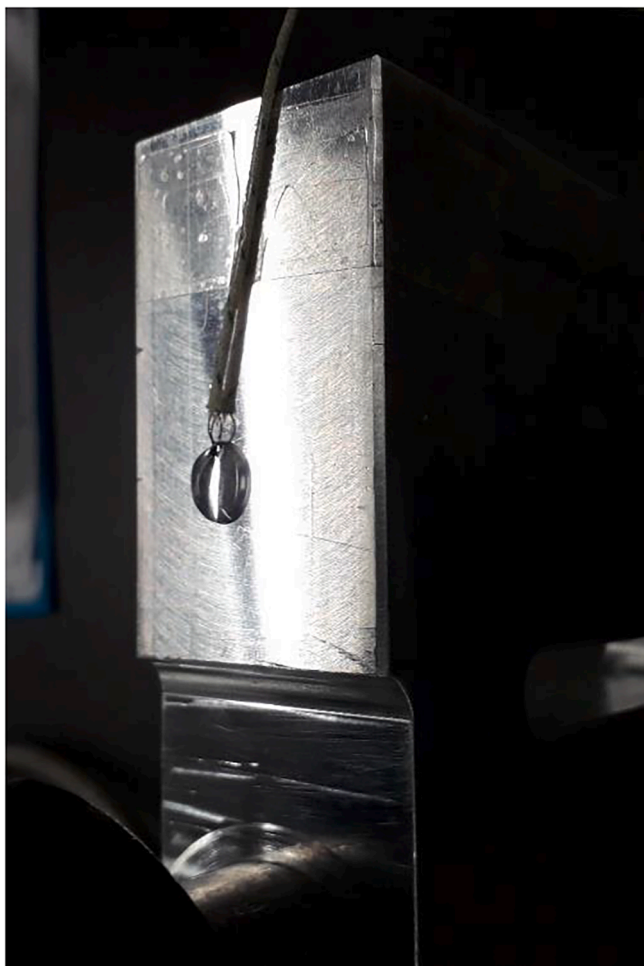


Fig. 10. Temperature measurement of the vibrating water drops.



Fig. 11. Temperature (left) and surface tension (right) measurement of SDBS dissolutions.

amplitude values can be considered for the discussion.

Analysing the frequency spectrum of the signal, it has been concluded that the vibration frequency was exactly 20 196 Hz.

Regarding the thermodynamic models, three different fluids have been tested. Each of them has different physical properties, summarized in Table 2.

For each fluid, the contact angle variation has been measured for different ultrasonic amplitude regimes with an average accuracy of \pm

Table 1

Peak to peak (PP) amplitude and null to peak (NP) amplitude for different ultrasonic power sources.

Power [%]	PP amplitude [μm]	NP amplitude [μm]
20	3.8	1.9
40	4.8	2.4
60	5.8	2.9
80	6.8	3.4
100	9.6	4.8

Table 2

Properties of the studied fluids.

	Density [kg/m^3]	Surface tension [N/m]	Viscosity [Pas]
Distilled water	1000	0.072	0.001
Ethylene glycol	1110	0.0477	0.0161
Glycerine	1260	0.0594	1.49

1.5 deg. After switching off the vibration, none of the experiments showed any regression in the contact line, which means that the contact angle hysteresis was strong enough to avoid the withdrawal of the droplet. The resolution of the goniometer was enough to observe the generation of capillary waves. In the case of distilled water, it has been observed that depending on the area where the droplets are deposited, capillary wave formation is more or less evident (Video S1). This behaviour can be explained by the fact that at high frequency, the resonance of the capillary wave depends strongly on the initial conditions (surface imperfections, initial contact angle, vibration heterogeneity, etc...). Fig. 12 shows the evolution of the contact angle for two different deposition points. In one case, capillary waves are visibly formed, in the other one not.

As can be noticed, when the capillary waves are not significant, the prediction and the real measurements for distilled water coincide quite well. However, significant capillary waves induce a deformation of the liquid–vapour interphase, and therefore the contact angle is not sufficiently reduced. The previous behaviour is not observed in high viscosity fluids such as ethylene glycol and glycerine. Both fluids tend to absorb part of the vibration energy as internal heating, which is why no capillary waves were observed. As shown in Fig. 13, the model without energy losses and the reality do not coincide. However, introducing a proportional loss factor of 0.28 [-] in the input amplitude, the model fits the reality with even better precision than distilled water.

The same experiment has been performed for glycerine, which is 160 times more viscous than ethylene glycol (Fig. 14). However, a slightly higher damping factor of 0.33 was needed to fit the models. This is a very interesting behaviour that can be explained by the fact that ethylene glycol is a non-Newtonian fluid that increases its apparent viscosity when shearing forces are applied [22]. The acoustic field is obviously introducing shearing forces, and therefore the apparent viscosity of this liquid turns to be similar to the one of glycerine, which is a Newtonian fluid.

The simplified theoretical model assumes that the ultrasonic heating (internal friction) is not enough to significantly increase the temperature of the fluid, as the surface tension would change otherwise.

As can be seen in Fig. 15, ultrasound was activated after second 10. The distilled water and the ethylene glycol droplets increased their internal temperature less than 0.7 °C after 20 s of exposure. This temperature change (0.7 °C) is not relevant regarding the surface tension of any of the fluids [23]. In conclusion, the assumption that the surface tension is not modified during the process is valid.

It can be concluded both analytically and experimentally that ultrasonic vibration can significantly increase wettability of three-phased wetting systems. Viscosity and capillary wave formation are significant attenuation factors, but if the contact angle hysteresis is strong enough to retain the contact line without withdrawal, the contact angle will

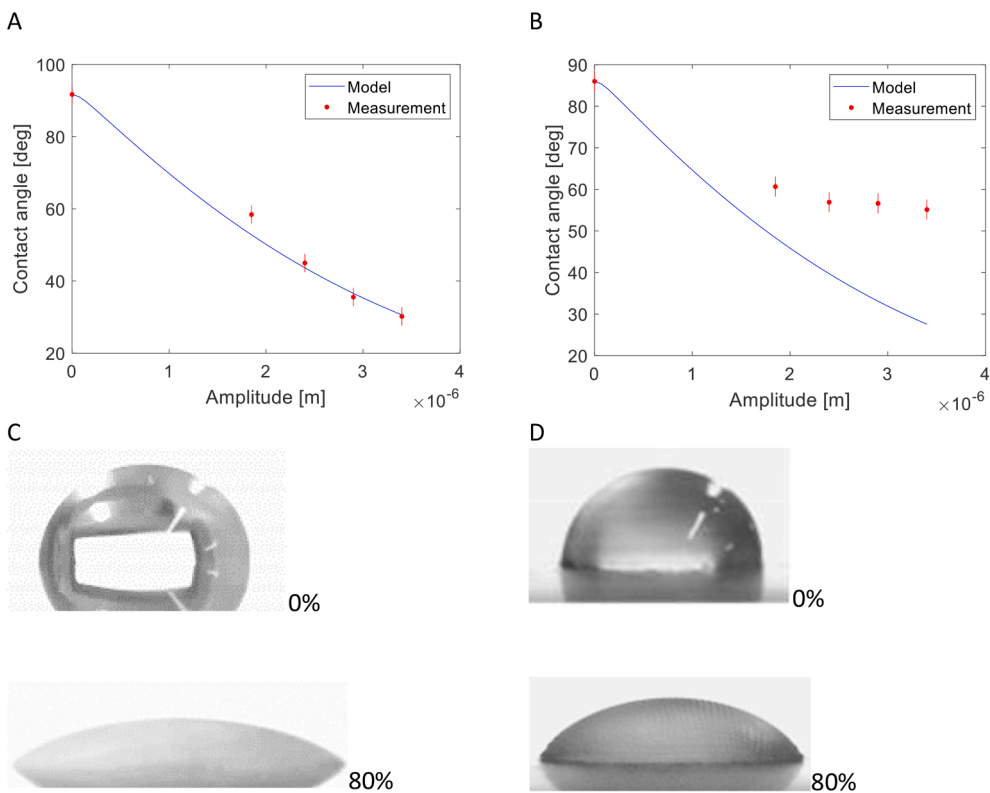


Fig. 12. A and C show the contact angle evolution from 0% of ultrasonic power to 80% respectively. B and D show the same evolution for visible capillary waves.

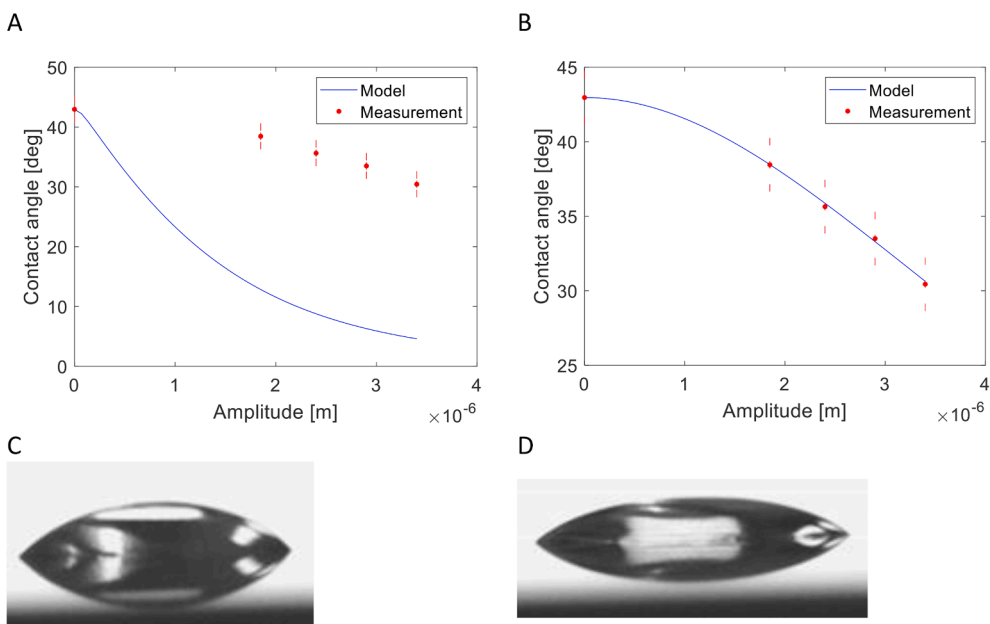


Fig. 13. A and B show the analytical prediction for ethylene glycol without and with damping factor, respectively. C shows the initial contact angle and D, at 80% of the power.

decrease. This phenomenon could have important industrial applications where conventional methods such as heat and surfactants prevail. Heating up a liquid to increase its wettability is the oldest method used by human being. Temperature modifies the surface tension of the liquids, and this is the reason why hot water cleans better than cold one. Surfactants also reduce the surface tension of the liquids, but they are based in chemical principles (amphiphilic molecules) not in thermal ones.

4.2. Energetic comparison: ultrasonic vibration

By using the previous thermodynamic models (Eq. (9)), it can be quantified how much ultrasonic energy is needed to reach a certain contact angle decrease. Table 3 shows the amount of ultrasonic energy needed for different degrees of the latter. As can be observed, the energetic values to obtain a significant contact angle reduction are below microjoule levels.

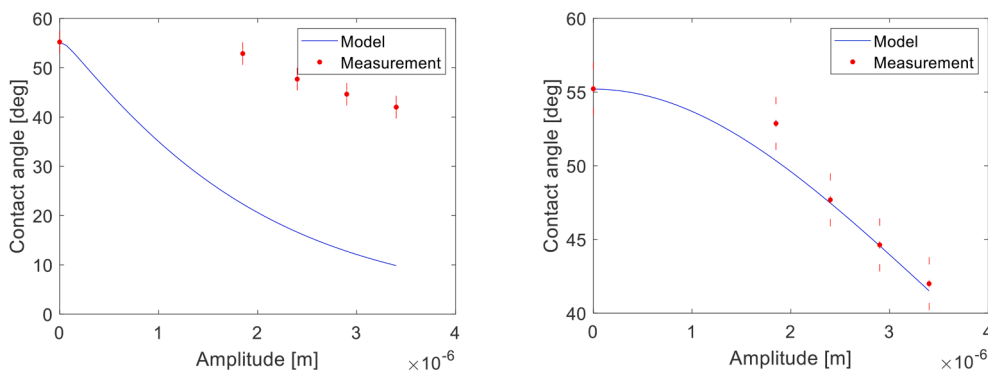


Fig. 14. Figures A and B show the analytical prediction for glycerine without and with damping factor.

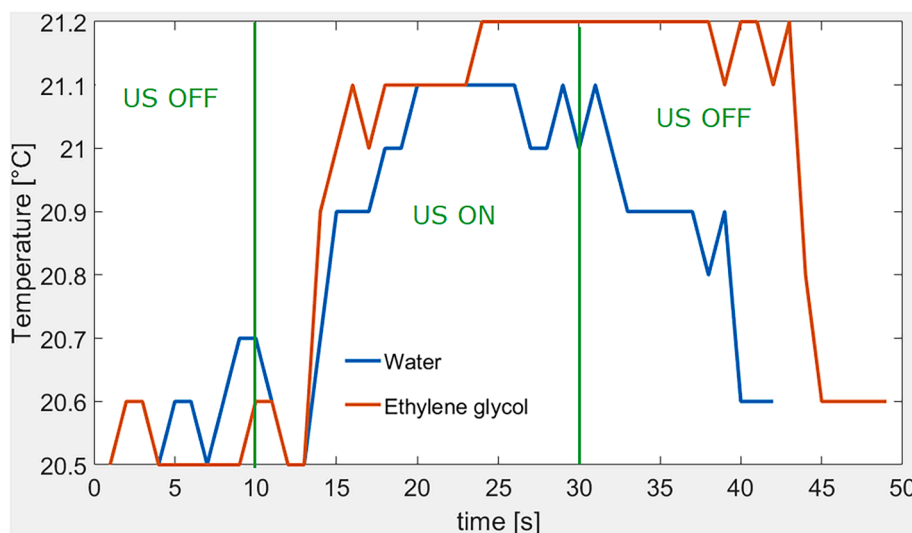


Fig. 15. Temperature [°C] evolution during time [s] under 100% of ultrasonic power. Vibration was activated at second 10 and deactivated at second 30. The blue line is for distilled water and the orange one for ethylene glycol. (For interpretation of the references to colour in this figure legend, the reader is referred to the web version of this article.)

Table 3

Minimum ultrasonic energy needed to reduce the contact angle for 5ul of distilled water on an aluminium plate.

$\Delta\theta$ [Deg]	ΔU [J]
10	6.801×10^{-09}
20	2.94×10^{-08}
30	7.297×10^{-08}
40	1.467×10^{-07}

4.3. Energetic comparison: heat

The dependency of contact angle with temperature has been measured by heating up the substrate and measuring the temperature and contact angle of the droplet deposited on it (Fig. 16)

If the thermal properties of the liquid (water) and its mass m are known, the absorbed heat Q [J] can be calculated through Eq. (12) (Table 4), where C is the specific heat capacity of the liquid phase and ΔT is the temperature increase:

$$Q = mC\Delta T \tag{13}$$

Applying a linear regression to the relationship between temperature and contact angle, one can conclude that 0.38 [J] of thermal energy are needed for 20 degrees of contact angle decay. Compared to the

ultrasonic method, thermal energy is about 8 orders of magnitude higher than the ultrasonic one. From the thermodynamic point of view, entropy is defined as “the measure of a system’s thermal energy per unit temperature that is unavailable for doing useful work”, so the difference between the ultrasonic and thermal method can be attributed to the higher generation of entropy of thermal one.

4.4. Energetic comparison: chemical surfactant

Finally, the use of surfactant (SDBS) has been evaluated from the energetic point of view. 6 different water + SDBS concentrations have been prepared and the contact angle and surface tension of each one have been measured on the aluminium substrate.

From Table 5 can be concluded, on the one hand, that the relationship between contact angle and SDBS concentration is not linear, nor the resulting surface tension. Indeed, both variables present a saturation point. This point is known as the critical micelle concentration CMC, where no more surfactant can migrate to the surface of the liquid and micelles are formed in the bulk [24]. Before reaching this point, the chemical potential of the SDBS is released during the dissolution. The Gibbs-Duhem Eq. (13) relates the chemical, entropic and surface tension dependence:

$$SdT + Ad\gamma + \sum_i n_i d\mu_i = 0 \tag{14}$$

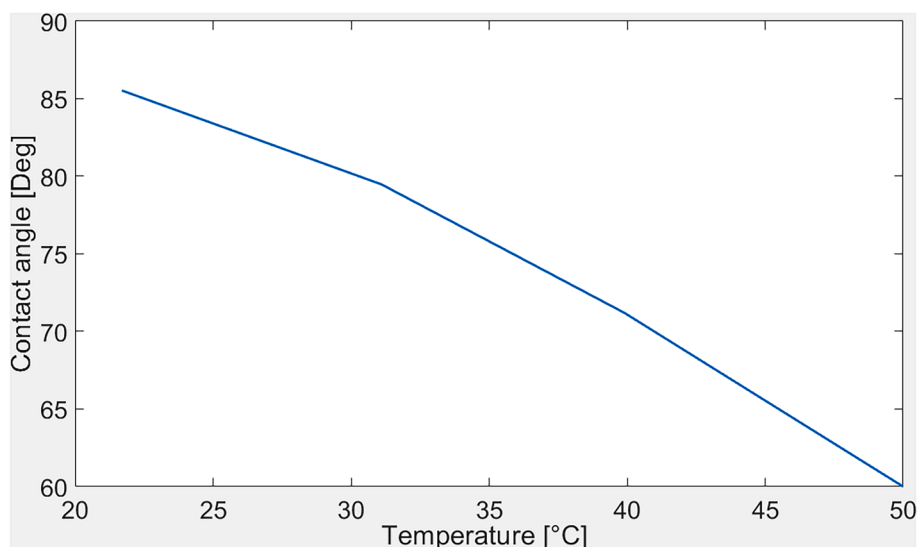


Fig. 16. Contact angle for different temperatures (distilled water).

Table 4
Contact angle decrease for different thermal energies (Q).

$\Delta\theta$ [Deg]	Q [J]
6.05	0.196
14.33	0.381
25.53	0.591

Table 5
Contact angle decrease for different SDBS + distilled water concentrations.

SDBS mass [%]	Contact angle [Deg]	Surface tension [N m ⁻¹]
0	74.53	68.5
0.05	56.88	38.1
0.1	48.94	32.2
0.3	35.1	32.2
1	30	30.8
3	30	30.5

If there are no temperature changes, the chemical potential of the surfactant will lead to the reduction of the surface tension of the dissolution. The temperature increase has been measured during the dissolution, and no changes were observed. It can therefore be considered that the chemical energy introduced by the SDBS is fully transformed into the surface stress reduction and therefore, into contact angle decrease.

$$dU = - \sum_i n_i d\mu_i = A d\gamma \tag{15}$$

And considering that the total surface energy is the half of the internal cohesion energy, it can be concluded that:

$$\Delta U = 2\Delta\gamma A \tag{16}$$

Table 6
Contact angle decrease for different chemical energy values.

$\Delta\theta$ [Deg]	ΔU [J]
17.65	8.59712×10^{-06}
25.59	1.02656×10^{-05}
39.43	1.02656×10^{-05}
44.53	1.06616×10^{-05}
44.53	1.07464×10^{-05}

Table 6 shows the relationship between contact angle decrease and chemical energy increase.

Interpolating the values of Table 6, it can be concluded that for 20 degrees of contact angle decay, 4.82×10^{-07} [J] of SDBS chemical energy are needed, which is slightly higher than in the case of ultrasonic energy.

From a molecular point of view, each method works in a very different way, as follows:

- Heat or thermal energy is, by definition, the amount of kinetic energy of the individual particles. Therefore, heat can be considered as atomic vibration. If this vibration is increased, the cohesion forces between the atoms will be reduced, and therefore, the surface stress and the contact angle.
- Ultrasonic vibration behaves in a similar way to heat, but at macroscopic level. The main difference is that there is no temperature increase and subsequent surface stress reduction.
- Chemical surfactants directly affect the surface of the droplet through the inclusion of amphiphilic molecules in the air-water interface. This method is therefore based in permanent change of the molecular structure of the droplet surface.

Table 7 summarizes the energy needed to change the contact angle in 20° for each approach. On the one hand, heat is by far the most energy demanding method. As mentioned, most part of the thermal energy is stored as internal entropy. Compared to ultrasonic vibration, the energy costs of heat are 7 orders of magnitude higher, and if the liquid is exposed to a colder atmosphere, heat will dissipate. In this sense, ultrasonic vibration and heat behave in a similar way. If the energy emitting source is switched off, the energy will be dissipated in the environment, but due to the hysteresis, the final contact angle will remain. The energy dissipation ratio is not the same for each case. Heat dissipation depends on convection and conduction, while sound is mechanically transmitted to the air or internally damped [1]. In any case, ultrasound will always dissipate much faster than heat. This is a

Table 7
Summary of the three approaches to reduce the contact angle in 20°.

Method	ΔU [J]
Ultrasonic (mechanical)	2.94×10^{-08}
Heat	0.38
SDBS (chemical)	4.82×10^{-07}

drawback for the implementation of the ultrasonic method as it must always be applied *in situ*. Unlike with heat and chemicals, it is not possible to apply ultrasound to a liquid in a recipient and pour it on the solid surface afterwards. On the other hand, SDBS and ultrasonic vibration need similar amounts of energy, but the chemical approach leads to a permanent change, while ultrasound does not. The main advantage of this permanent change is that once the dissolution is done, there is no energy dissipation, and therefore the chemical method needs, in practice, less energy. Nevertheless, the resulting fluid is the mixture of two components (surfactant and water), which implies several environmental drawbacks. Depending on the kind of surfactant, it might be harmful for water micro-organisms [25]. The current trend is to use bio-based surfactants that do not affect the environment. Even so, drinkable water is a critical issue for many countries [26], so the usage of water and surfactant dissolution should be reduced in processes such as cleaning.

Its combination of low energy consumption and no environmental pollution make ultrasonic methods the most environmentally friendly approach for wettability increase. Unlike traditional methods or surface texturing, ultrasound can instantly modulate the contact angle, and the effect is reversible.

5. Conclusions and outlook

The present work develops a novel thermodynamical approach to explain the reason why high frequency vibration increases the wettability in three-phase systems. The main mechanism is based on the combination of the vibration driving force and the contact angle hysteresis. A mathematical model has been programmed and validated with real measurements. The vibration method has been energetically compared with conventional heating and chemical surfactants. The main conclusions of the work are:

- In wetting systems, ultrasonic vibration decreases the contact angle with no return. For a fixed frequency, the contact angle decay depends on the ultrasonic amplitude.
- For low viscosity liquids such as water, the presence of capillary waves reduces the wettability enhancement. This effect could be explained by the fact that the capillary waves stretch the surface of the liquid decreasing its expansion.
- When the model is applied to viscous liquids (ethylene glycol and glycerine), damping factors must be included in the formulation. At high frequency, non-Newtonian fluids such as ethylene glycol need lower damping ratios.
- After 30 s of ultrasonic exposure, the temperature of the droplets only increases by 0.6 °C, which is not enough to relate the contact angle decrease with the surface tension drop induced by temperature.
- Thermal wettability enhancement (reduction of surface stress) is the most energy-demanding method. Compared to ultrasound or surfactants, the consumed energy is 8 orders of magnitude higher.
- The energy consumed by surfactants (SDBS) is slightly higher than with ultrasonic vibration, but the effect is permanent. However, environmental issues must be considered for this method.
- As mechanical energy, ultrasonic vibration is the most energy-efficient. The main drawback of the technology is that it must be applied *in situ*.
- The ultrasonic approach is unique, as it allows to instantly tune the contact angle.

Ultrasonic wettability tuning has been mainly discussed and compared for the case of distilled water, but further studies should take place to analyse the reaction times and accuracy of the method. In the same way, the interaction between the effect of capillary waves and

droplet stretching could be analysed through CFD simulation. This could be a key to reverse the process by generating an ultrasonic hydrophobic effect.

There is a wide field of applications related to the wettability and contact angle, such as tuneable surfaces and microfluidics.

Declaration of Competing Interest

The authors declare that they have no known competing financial interests or personal relationships that could have appeared to influence the work reported in this paper.

Acknowledgments

The projects leading to this research have received funding from the European Union's Horizon 2020 research and innovation programme under grant agreement N° 654479 WASCOP and N°792103 SOLWARIS.

References

- [1] J.A. Gallego-Juárez, K.F. Graff, *Power ultrasonics: applications of high-intensity ultrasound*, Elsevier, 2014.
- [2] W. Lauterborn, T. Kurz, R. Mettin, C.D. Ohl, *Experimental and theoretical bubble dynamics*, *Adv. Chem. Phys.* 110 (1999) 295–380.
- [3] W. Lauterborn, T. Kurz, R. Geisler, D. Schanz, O. Lindau, *Acoustic cavitation, bubble dynamics and sonoluminescence*, *Ultrason. Sonochem.* 14 (4) (2007) 484–491.
- [4] J.T. Tervo, R. Mettin, W. Lauterborn, *Bubble cluster dynamics in acoustic cavitation*, *Acta Acust. united with Acust.* 92 (1) (2006) 178–180.
- [5] T.J. Mason, *Ultrasonic cleaning: An historical perspective*, *Ultrason. Sonochem.* 29 (2016) 519–523.
- [6] M.A. Trapuzzano, "Controlled Wetting Using Ultrasonic Vibration," 2019.
- [7] BOJAN VUKASINOVIC, MARC.K. SMITH, ARI GLEZER, *Dynamics of a sessile drop in forced vibration*, *J. Fluid Mech.* 587 (2007) 395–423.
- [8] H. Lamb, "Hydrodynamics, Cambridge Univ", Press, 1932, pp. 134–139.
- [9] L. Dong, A. Chaudhury, M.K. Chaudhury, *Lateral vibration of a water drop and its motion on a vibrating surface*, *Eur. Phys. J. E* 21 (3) (2006) 231–242.
- [10] A. Tamura, *Surface vibrations of a He 4 droplet and the universality of the dispersion relation*, *Phys. Rev. B* 53 (21) (1996) 14475.
- [11] R.J. Lang, *Ultrasonic atomization of liquids*, *J. Acoust. Soc. Am.* 34 (1) (1962) 6–8.
- [12] R. Pohlman, K. Heisler, M. Cichos, *Powdering aluminium and aluminium alloys by ultrasound*, *Ultrasonics* 12 (1) (1974) 11–15.
- [13] V. I. Sorokin, "The effect of fountain formation at the surface of a vertically oscillating liquid," *Sov. Phys. Acoust.*, vol. 3, no. 281, 1957.
- [14] A. Lozano, J. A. Garcí\ia, J. Alconchel, F. Barreras, E. Calvo, and J. L. Santolaya, "Influence of liquid properties on ultrasonic atomization," 2017.
- [15] M. Costalonga, P. Brunet, *Directional motion of vibrated sessile drops: A quantitative study*, *Phys. Rev. Fluids* 5 (2) (2020) 23601.
- [16] T. Urai, M. Kamai, H. Fujii, *Estimation of intrinsic contact angle of various liquids on PTFE by utilizing ultrasonic vibration*, *J. Mater. Eng. Perform.* 25 (8) (2016) 3384–3389.
- [17] M. Morozov, O. Manor, *Vibration-driven mass transfer and dynamic wetting*, *Curr. Opin. Colloid Interface Sci.* 36 (2018) 37–45.
- [18] Q. Lin, C. Xing, R. Sui, W. Ci, Y. Xu, *Effect of ultrasonic vibration on wetting of water/Cu, water/PTFE, E-GaN/Cu and E-GaN/graphite*, *Exp. Therm. Fluid Sci.* 102 (2019) 351–356.
- [19] O. Manor, M. Dentry, J.R. Friend, L.Y. Yeo, *Substrate dependent drop deformation and wetting under high frequency vibration*, *Soft Matter* 7 (18) (2011) 7976–7979.
- [20] M. Trapuzzano, A. Tejada-Martínez, R. Guldiken, N. Crane, *Volume and Frequency-Independent Spreading of Droplets Driven by Ultrasonic Surface Vibration*, *Fluids* 5 (1) (2020) 18, <https://doi.org/10.3390/fluids5010018>.
- [21] A.I. Rusanov, N.E. Esipova, V.D. Sobolev, *Strong dependence of contact angle on pressure*, *Doklady Physical Chemistry* 487 (1) (2019) 87–90.
- [22] K. Yapici, O. Osturk, Y. Uludag, *Dependency of nanofluid rheology on particle size and concentration of various metal oxide nanoparticles*, *Brazilian J. Chem. Eng.* 35 (2) (2018) 575–586.
- [23] C. Gianino, *Measurement of surface tension by the dripping from a needle*, *Phys. Educ.* 41 (5) (2006) 440–444.
- [24] K.A. Moharram, M.S. Abd-Elhady, H.A. Kandil, H. El-Sherif, *Influence of cleaning using water and surfactants on the performance of photovoltaic panels*, *Energy Convers. Manag.* 68 (2013) 266–272.
- [25] T. Ivanković, J. Hrenović, *Surfactants in the environment*, *Arch. Ind. Hyg. Toxicol.* 61 (1) (2010) 95–110.
- [26] S. Bouaddi, A. Fernández-García, C. Sansom, J. Sarasua, F. Wolfertstetter, H. Bouzekri, F. Sutter, I. Azpitarte, *A review of conventional and innovative-sustainable methods for cleaning reflectors in concentrating solar power plants*, *Sustainability* 10 (11) (2018) 3937, <https://doi.org/10.3390/su10113937>.